ChemComm

COMMUNICATION

View Article Online
View Journal | View Issue

Cite this: *Chem. Commun.*, 2014, **50**, 11825

Received 16th July 2014,
Accepted 13th August 2014

DOI: 10.1039/c4cc05482b

www.rsc.org/chemcomm

On-surface aryl–aryl coupling *via* selective C–H activation†

Qiang Sun, Chi Zhang, Huihui Kong, Qinggang Tan and Wei Xu*

Through the interplay of high-resolution scanning tunneling microscopy (STM) imaging/manipulation and density functional theory (DFT) calculations, we have demonstrated that an unprecedented selective aryl–aryl coupling *via* direct C–H bond activation can be successfully achieved on Cu(110). These findings present a simple and generalized route for preparing low dimensional carbon nanomaterials.

The carbon–carbon coupling reaction through direct C–H activation has long remained as one of the most challenging topics in chemical science due to the relative inertness and poor selectivity of C–H bonds. Tremendous efforts have been devoted in this field and many strategies, for example, use of transition metal catalysts, harsh conditions and metal surfaces, have been employed for activating C–H bonds.[1–4] Recently, metal surfaces have been employed as platforms and heterogeneous catalysts have been used to facilitate a variety of well-known chemical reactions under ultra-high vacuum conditions or in solution. For instance, Ullmann coupling, Bergman cyclization, imine coupling, click reactions and Glaser coupling have been successfully introduced on different metal surfaces.[5–15] Moreover, recent studies have illustrated that an unexpected reaction, that is, C–C coupling of alkane molecules *via* C–H activation can also be successfully achieved on metal surfaces.[16,17] As mentioned above, investigation on the feasibility of C–C coupling of other typical hydrocarbons *via* direct C–H activation on metal surfaces is of utmost importance, especially, activating the C–H bond of arenes should be particularly interesting as aryl groups are the principal components of aromatic molecules. Previous studies have shown that the intramolecular aryl–aryl coupling could occur where the reactions took place in very confined environments,[5,18,19] whereas, intermolecular aryl–aryl coupling *via* C–H activation has so far been rarely reported. It is therefore of tremendous interest to investigate the aryl–aryl coupling *via* C–H activation between free molecules on metal surfaces where, importantly, the selectivity of C–H activation could be explored in depth.

To explore the above mentioned aryl–aryl coupling *via* C–H activation on the surface, we have in this study chosen a simple and representative aromatic molecule, the quaterphenyl (4Ph) molecule, which is a linear molecule consisting of four σ-bonded phenyl rings and is generally investigated for preparation of ordered organic films by weak intermolecular interactions on surfaces.[20,21] The anisotropic Cu(110) surface is employed as a platform to heterogeneously catalyze the on-surface aryl–aryl coupling due to the relatively high chemical activity and the well-known 1-D templating effect of the substrate.[7,22] Here, through the interplay of high-resolution scanning tunneling microscopy (STM) imaging/manipulation and density functional theory (DFT) calculations, we demonstrate that 4Ph molecules initially form a two-dimensional (2-D) close-packed structure after direct deposition on the surface held at room temperature (RT), whereas, upon heating up the surface to 500 K, surprisingly, we find that the 4Ph molecules are covalently linked together *via* aryl–aryl coupling into chain-like structures basically along the close-packed [1–10] direction of the substrate. Moreover, interestingly, submolecularly resolved STM images reveal that the aryl–aryl coupling takes place at the specific site of the terminal phenyl groups of 4Ph molecules exclusively, which is further confirmed by delicate lateral STM manipulations. The DFT calculations on the energy barriers of all possible C–H activation sites within the 4Ph molecule elucidate this unexpected selective aryl–aryl coupling process, and also well explain the scenario for the formation of the resulting chain-like structures with certain structural motifs on the Cu(110) surface. These unprecedented findings demonstrate a novel surface chemistry method for selectively activating the C–H bonds of aromatic molecules, and moreover may present a simple and generalized route for preparing low dimensional carbon nanomaterials like graphene nanoribbons on surfaces without special efforts in functionalizing molecular precursors.

As shown in Fig. 1, the 4Ph molecules form a close-packed structure with unidirectional molecular arrangement after

---

College of Materials Science and Engineering, Tongji University, Caoan Road 4800, Shanghai 201804, P. R. China. E-mail: xuwei@tongji.edu.cn

† Electronic supplementary information (ESI) available. See DOI: 10.1039/c4cc05482b

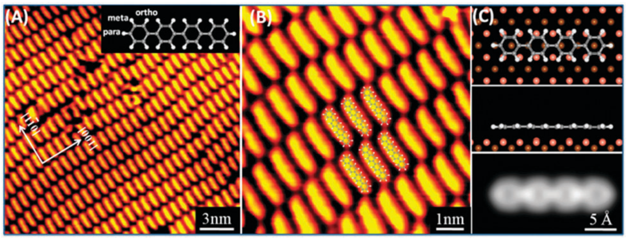

Fig. 1 (A) Large-scale and (B) close-up STM images of 4Ph molecules arranged on Cu(110) at a high molecular coverage. The chemical structure of the 4Ph molecule is shown in the inset in (A) where the *ortho*-C, *meta*-C and *para*-C sites of the terminal phenyl group are given. (C) The top-view (upper panel) and the side-view (middle panel) of the DFT-relaxed model of the 4Ph molecule on Cu(110), and the corresponding STM image simulation (lower panel) at the bias voltage of −1500 mV. Scanning conditions: I_t = 0.8 nA, V_t = −1500 mV.

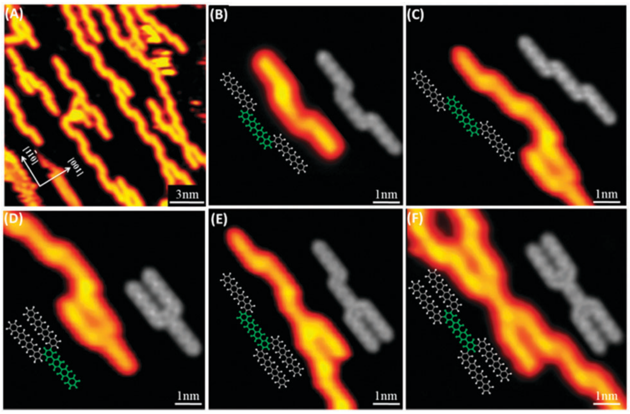

Fig. 2 (A) STM image showing the formation of chain-like structures with branches after annealing the 4Ph-covered surface at a low molecular coverage at 500 K. (B)–(F) The close-up STM images, the equally-scaled optimized structural models and the DFT-based STM image simulations (the black and white ones) of the typical structural motifs within the chain structures. One of the 4Ph molecules shown in the models is colored in green in order to illustrate how the different structural motifs are derived from it. The structural motifs are formed by different numbers of linked molecules or positions of *meta*-C sites based on the 4Ph molecule colored in green in the models of (B)–(F). Scanning condition: I_t = 0.75 nA, V_t = −2500 mV. The STM image simulations are performed at the bias voltage of −2500 mV.

deposition on Cu(110) at RT with a relatively high coverage.[23,24] 4Ph molecules tend to align with their long axes along the [1–10] direction of the substrate and the equivalently scaled molecular models are superimposed in the close-up STM image, as shown in Fig. 1B. Fig. 1C shows the DFT optimized adsorption geometry of the 4Ph molecules on Cu(110) where a flat-lying geometry is adopted as other planar π-conjugated molecules on surfaces.[25,26] The DFT-based STM simulation of 4Ph molecules is also carried out to further verify the experimental findings. Note that owing to a lack of strong and directional intermolecular interactions between the molecules, the molecular arrangement is not perfectly ordered.

After annealing the 4Ph-covered sample at 500 K, we surprisingly find that the 4Ph molecules are linked together into chain-like structures basically along the close-packed [1–10] direction of the substrate, as shown in Fig. 2A. A closer inspection of the STM image shows that there are also some branches derived from the chain structures, and further discloses that the chain structures could be recognized as the combination of one building block which is consistent with the 4Ph monomer in dimension and the STM profile. Moreover, we could identify that the majority of 4Ph molecules are joined together in a uniform shoulder-to-shoulder fashion. Detailed analysis of STM images allowed us to distinguish the typical structural motifs within the chain-like structures as singled out in Fig. 2B–F which show close-up high-resolution STM images. From the close-up STM images we can identify that the electronic density of states at the molecular junctions is rather smooth and seamless which is a characteristic feature of covalent linkages between organic molecules on surfaces.[5,8,9] We then naturally speculated that the on-surface aryl–aryl coupling takes place between 4Ph molecules when we heat up the sample to 500 K. On the basis of the above analyses, we carried out extensive theoretical calculations based on the DFT method, and the equally scaled optimized structural models were compared with the corresponding STM images accompanied by the DFT-based STM image simulations, where excellent agreements were achieved. As indicated in the proposed models shown in Fig. 2B–F, we can distinguish that the aryl–aryl coupling between 4Ph molecules takes place at the *meta*-C sites of the terminal phenyl groups exclusively. Note that the involvement of the copper atom in the chain structure should be ruled out as the metal atoms normally show pronounced protrusions in the C–Cu–C linkage in STM images[13,27,28] and the disagreement of the intermolecular distance within the chain. (*cf.* Fig. S1, ESI†).

To further verify the selective aryl–aryl coupling between 4Ph molecules, we performed a series of delicate lateral STM manipulations. The manipulations were carried out in a controllable line-scan mode by increasing the tunnel current up to ∼2.0 nA and reducing the tunnel voltage down to ∼20 mV.[29,30] As shown in Fig. 3, after manipulating a molecular chain along the blue arrow as indicated, we find that the chain structure remains unbroken, while, more interestingly, the orientation of the uppermost molecule is changed to a certain degree with respect to its original position. As illustrated by the overlaid molecular models on the STM images and the schematic models, we can clearly see that the molecular orientation change is induced by the rotation about the newly formed C–C σ-bond (the green one indicated in

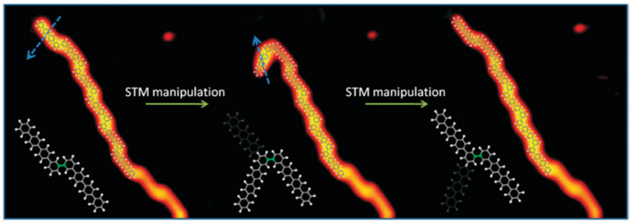

Fig. 3 Two sequential lateral STM manipulations of the molecular chain show that the orientations of the uppermost molecule could be reversibly switched just between two certain degrees. The blue arrows indicate the directions of STM manipulations. The schematic models demonstrate how the molecular orientations are changed and recovered.

the schematic models) at the *meta*-C sites between the 4Ph molecules, as proposed above. Furthermore, the changed molecular orientation is recovered after another STM manipulation shown in Fig. 3, and this reversible switch of molecular orientations just between two certain degrees could be repeated several times and the molecular chain is still intact, which undoubtedly confirms the covalent nature of the molecular chain, and moreover provids a solid evidence of the selective aryl–aryl coupling at the specific C sites between 4Ph molecules.

Such unexpected selective aryl–aryl coupling at specific sites results in the observed shoulder-to-shoulder joining and furthermore the formation of certain structural motifs demonstrated in Fig. 2B–F. Based on these structural motifs the whole chain-like structures are then built up, and the directionality of the chains is induced by the 1-D templating effect of the Cu(110) substrate. Note that further experiments (with different surface coverage) illustrate that the number of branches within chain-like structures increases at higher molecular coverage (*cf.* Fig. S2, ESI†), and the typical structural motifs remain the same indicating that the selectivity of aryl–aryl coupling does not depend on the molecular coverage. Moreover, we performed a thorough statistical analysis of the relative occurrence of different structural motifs at low and high coverage (*cf.* Fig. S3, ESI†).

To unravel this unexpected selectivity of aryl–aryl coupling between 4Ph molecules on Cu(110), systematic DFT calculations including the substrate were performed. As shown in Fig. 4A, we calculated the energy barriers of all possible C–H activation sites (denoted as C_1, C_2, C_3, C_4 and C_5 in the schematic model, other sites are identical with respect to these five) within the 4Ph molecule on Cu(110). From the energy diagrams we could clearly identify that C–H activation at the specific C_2 site (the *meta*-C site mentioned before) is energetically most favorable (with a barrier of ∼1.7 eV), demonstrating that the 4Ph molecules tend to dehydrogenate and link together preferentially at C_2 sites, which well accounts for the experimentally observed selective aryl–aryl coupling. Here, the registry between the molecule and the substrate may be responsible for the energy differences among different C sites.

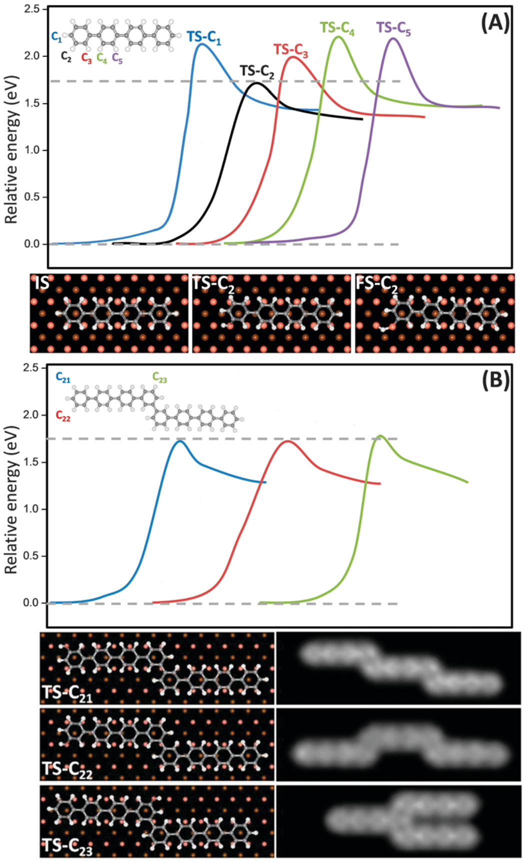

Fig. 4 (A) DFT-calculated energy diagrams for C–H activation of 4Ph molecule at five different sites (denoted as C_1, C_2, C_3, C_4 and C_5, respectively) on Cu(110). The structural models of the initial state (IS), the transition state (TS-C_2) and the final state (FS-C_2) of the energetically lowest pathway are shown below the energy diagrams. All the other corresponding structural models are shown in Fig. S4, ESI.† (B) DFT-calculated energy diagrams for C–H activation of 4Ph molecular dimer at three different sites (denoted as C_{21}, C_{22} and C_{23}, respectively) on Cu(110). The structural models of the respective transition states (TS-C_{21}, TS-C_{22} and TS-C_{23}) and the corresponding resulting 4Ph trimers indicated by STM image simulations are shown below the energy diagrams.

To elucidate the mechanism of the formation of the chain-like structures observed experimentally, we performed further DFT calculations in a more complicated situation. Then, calculations on the C–H activation energy barriers of three sites from a dimer structure (denoted as C_{21}, C_{22} and C_{23} in the schematic model) are carried out to explore the possible formation process of trimers or even larger structural motifs, as shown in Fig. 4B. From the energy diagrams we can identify that the energy barriers of C–H activation at the sites C_{21}, C_{22} and C_{23}, respectively, are the same as the barrier of C–H activation at the C_2 site of the 4Ph monomer on Cu(110). Based on the experimental and theoretical results we now propose the following scenario for the formation of the observed chain-like structures: (1) first, dehydrogenation selectively occurs at one of the identical C_2 sites of a 4Ph monomer upon gaining enough energy, and subsequently two dehydrogenated monomers prefer to form a dimer structure by aryl–aryl coupling; (2) then one of the identical C_{21}, C_{22} and C_{23} sites of the dimer structure dehydrogenates to facilitate the formation of certain structural motifs as mentioned above and further the extension to the chain-like structures. Note that the mechanism of the selective coupling is different from that reported in a previous work on on-surface selective coupling.[31,32]

In conclusion, through high-resolution UHV-STM imaging/manipulation and detailed DFT calculations, we have demonstrated that an unprecedented selective aryl–aryl coupling *via* direct C–H bond activation can be successfully achieved on Cu(110), which exhibits the intriguing potential of surface chemistry. These novel findings may suggest a relatively simple and generalized route for selectively activating the C–H bond of aromatic molecules, and may also shed light on fabricating low dimensional carbon nanomaterials *via* direct aryl–aryl coupling without functionalizing molecular precursors or preparing complicated catalysts.

The authors acknowledge the financial support from the National Natural Science Foundation of China (21103128), the Shanghai "Shu Guang" Project supported by the Shanghai Municipal Education Commission and Shanghai Education Development Foundation (11SG25), the Fundamental Research Funds for the Central Universities, the Research Fund for the Doctoral Program of Higher Education of China (20120072110045).

Notes and references

1 D. H. Wang, T. S. Mei and J. Q. Yu, *J. Am. Chem. Soc.*, 2008, **130**, 17676.

2 L. Yin and J. Liebscher, *Chem. Rev.*, 2007, **107**, 133.

3 J. H. Lunsford, *Catal. Today*, 2000, **63**, 165.

4 B. A. Arndtsen, R. G. Bergman, T. A. Mobley and T. H. Peterson, *Acc. Chem. Res.*, 1995, **28**, 154.

5 J. Cai, P. Ruffieux, R. Jaafar, M. Bieri, T. Braun, S. Blankenburg, M. Muoth, A. P. Seitsonen, M. Saleh, X. Feng, K. Mullen and R. Fasel, *Nature*, 2010, **466**, 470.

6 S. Weigelt, J. Schnadt, A. K. Tuxen, F. Masini, C. Bombis, C. Busse, C. Isvoranu, E. Ataman, E. Lægsgaard, F. Besenbacher and T. R. Linderoth, *J. Am. Chem. Soc.*, 2008, **130**, 5388.

7 Q. Sun, C. Zhang, Z. Li, H. Kong, Q. Tan, A. Hu and W. Xu, *J. Am. Chem. Soc.*, 2013, **135**, 8448.

8 G. Franc and A. Gourdon, *Phys. Chem. Chem. Phys.*, 2011, **13**, 14283.

9 L. Grill, M. Dyer, L. Lafferentz, M. Persson, M. V. Peters and S. Hecht, *Nat. Nanotechnol.*, 2007, **2**, 687.

10 F. Bebensee, C. Bombis, S. R. Vadapoo, J. R. Cramer, F. Besenbacher, K. V. Gothelf and T. R. Linderoth, *J. Am. Chem. Soc.*, 2013, **135**, 2136.

11 Y. Q. Zhang, N. Kepcija, M. Kleinschrodt, K. Diller, S. Fischer, A. C. Papageorgiou, F. Allegretti, J. Bjork, S. Klyatskaya, F. Klappenberger, M. Ruben and J. V. Barth, *Nat. Commun.*, 2012, **3**, 1286.

12 L. Lafferentz, V. Eberhardt, C. Dri, C. Africh, G. Comelli, F. Esch and L. Grill, *Nat. Chem.*, 2012, **4**, 215.

13 W. Wang, X. Shi, S. Wang, M. A. Van Hove and N. Lin, *J. Am. Chem. Soc.*, 2011, **133**, 13264.

14 X. Liu, C. Guan, S. Ding, W. Wang, H. Yan, D. Wang and L. Wan, *J. Am. Chem. Soc.*, 2013, **135**, 10470.

15 J. Björk and F. Hanke, *Chem. – Eur. J.*, 2014, **20**, 928.

16 D. Zhong, J. Franke, S. K. Podiyanachari, T. Blömker, H. Zhang, G. Kehr, G. Erker, H. Fuchs and L. Chi, *Science*, 2011, **334**, 213.

17 P. Iavicoli, S. Haq, D. B. Amabilino and R. Raval, *Chem. Commun.*, 2008, 1536.

18 M. Treier, C. A. Pignedoli, T. Laino, R. Rieger, K. Mullen, D. Passerone and R. Fasel, *Nat. Chem.*, 2011, **3**, 61.

19 G. Otero, G. Biddau, C. Sanchez-Sanchez, R. Caillard, M. F. Lopez, C. Rogero, F. J. Palomares, N. Cabello, M. A. Basanta, J. Ortega, J. Mendez, A. M. Echavarren, R. Perez, B. Gomez-Lor and J. A. Martin-Gago, *Nature*, 2008, **454**, 865.

20 S. Mullegger, I. Salzmann, R. Resel and A. Winkler, *Appl. Phys. Lett.*, 2003, **83**, 4536.

21 G. Witte and C. Woll, *J. Mater. Res.*, 2004, **19**, 1889.

22 M. Oehzelt, L. Grill, S. Berkebile, G. Koller, F. P. Netzer and M. G. Ramsey, *ChemPhysChem*, 2007, **8**, 1707.

23 W. Chen, H. L. Zhang, H. Huang, L. Chen and A. T. S. Wee, *Appl. Phys. Lett.*, 2008, **92**, 193301.

24 S. Lukas, G. Witte and C. Wöll, *Phys. Rev. Lett.*, 2001, **88**, 028301.

25 L. Dong, Q. Sun, C. Zhang, Z. Li, K. Sheng, H. Kong, Q. Tan, Y. Pan, A. Hu and W. Xu, *Chem. Commun.*, 2013, **49**, 1735.

26 L. Gross, F. Moresco, P. Ruffieux, A. Gourdon, C. Joachim and K. Rieder, *Phys. Rev. B: Condens. Matter Mater. Phys.*, 2005, **71**, 165428.

27 F. Hanke, S. Haq, R. Raval and M. Persson, *ACS Nano*, 2011, **5**, 9093.

28 S. Haq, F. Hanke, M. S. Dyer, M. Persson, P. Iavicoli, D. B. Amabilino and R. Raval, *J. Am. Chem. Soc.*, 2011, **133**, 12031.

29 W. Xu, H. Kong, C. Zhang, Q. Sun, H. Gersen, L. Dong, Q. Tan, E. Laegsgaard and F. Besenbacher, *Angew. Chem., Int. Ed.*, 2013, **52**, 7442.

30 M. Yu, W. Xu, Y. B. Jalal, E. Laegsgaard, I. Stensgaard, X. Bouju, A. Gourdon, C. Joachim, T. R. Linderoth and F. Besenbacher, *Nano Res.*, 2009, **2**, 254.

31 L. Lafferentz, V. Eberhardt, C. Dri, C. Africh, G. Comelli, F. Esch, S. Hecht and L. Grill, *Nat. Chem.*, 2012, **4**, 215.

32 M. Kittelmann, M. Nimmrich, R. Lindner, A. Gourdon and A. Kühnle, *ACS Nano*, 2013, **7**, 5614.